68

CODED PULSE RADAR

(CORRELATION RADAR USING RANDOMLY CODED PULSE)

Toshifusa Sakamoto, Yasuo Taki, Hiroshi Miyakawa, Hisashi Kobayashi, Tsutomu suzuki, Takeo Takeya, Takashi Yoshida and Mikio Kokubu

The conventional pulse radar has several shortcomings as a long range rader. Since the pulse width is constrained by resolution, the extention of the detection range is only accomplished by increasing the peak power of a transmitted pulse. As a consequence, in many situations, high power tubes are being used inefficiently as far as average power is concerned. It was realized early in the research program, that in order to obtain improved performances of the long range radar systems, not only must the wide pulse with large total power be used, but also the product of signal band-width and duration, that is, the radar response function, should be sharply defined and possess a low side-lobe lebll. These requirements, are listed on Fig. 1. In accordance with these requirements, a coded pulse radar was proposed as a long range radar and the laboratory experiments were carried on to demonstrate the principle of the coded pulse radar.

We are concerned with a long range radar which gives both range and doppler data. The system utilizes a rather wide transmitted pulse with a low repetition rate. A high range resolution is accomplished by modulating the phase of the carrier of transmitted pulse. Pseudeo-random sequence generated by using a feedback shift register is utilized as a molulating signal.

The basic block diagram of the transmitter is shown in Fig. 2. A wide RF pulse with the width of T generated from a crystal controlled oscillator is supplied to a phase modulator, where the carrier pulse is phase-modulated by a pseudo-random signal from a pseudo-random sequence generator. The signal waveforms involved in the diagram are shown in Fig. 3. The top figure shows the unmodulated R-F pulse, the second figure shows the pseudo-random sequence derived from a pseudo-random sequence generator, that is, a kind of a feedback shift register. The carrier pulse is modulated by the pseudo-random signal resulting to the third waveforms, that is the transmitted pulse, on this figure, 0° and 180° indicate the phase of modulated carrier relative to the phase of unmodulated carrier.

The basic block diagram of the receiver is shown in Fig. 4. At the receiver, the signal reflected from the target, is phase-modulated by the replica of the pseudo-random signal used in the transmitter. In the diagram, the first local reference signal means the replica of the pseudo-random signal without delay, the second local reference signal means the replica of the pseudo-random signal with one unit of delay which corresponds to one code element, in other words, one cycle of the feedback shift register, and in the same way the n-th local reference signal means the replica of the pseudo-random signal with delay of n -1 units.

The demodulated signal is supplied to the filter bank, which consists of a number of narrow band filters with bandwidth of 1/T. For the moving targets, the doppler effect produces frequency difference between the transmitted and received pulse. Since the doppler shift is not known a priori, we must be prepared to process an echo which occurs anywhere within the rather wide bandwidth. The filter bank serves to discriminate the reflected signals each other from the targets of different velocities.

And a number of local reference signals with different delays serve to discriminate the signals each other reflected from the targets of different positions Fig. 5 and 6 show the principle of position and velocity discrimination.

The signal waveforms involved in the detection process in case of zero time difference between the reflected signal and the local reference signal are shown in Fig. 5. In this case, the output of the phase modulator is a continuous wave without phase modulation. Suppose there is no doppler frequency shift, then the output of the first filter, in which signal appears, indicates the presence of a target. The other channels give only small outputs.

The signal waveforms involved in the detection process in case of non-zero time difference between the reflected signal and the local reference signal are shown in Fig. 6. In this case, the output of the phase modulator is a phase-modulated sinusoidal wave. Because the pseudo-random sequence is derived by the maximally-length feedback shift register, the number of the units of the plus phase of the demodulated waveform is almost equal to that of the minus phase. Because the plus phase and the minus phase cancell out each other, non of the filter outputs does not build up sufficiently. This is also explained by the fact that the spectrum of the output of the demodulator spreads over wide frequency ranges, while each filter of the filter bank has narrow bandwidth.

The outputs of the filter bank are supplied to envelope detectors. To extend the range of target detection further, we utilized the double threshold method of detection as a means of post-detection integration. Fig. 7 shows the basic principle of the double threshold method of detection.

The pseudo-random signal utilized to modulate the transmitted pu pulse has a period of T. that is, the transmitted pulse width. According to the simple theory of correlation detection, this prevents the unambiguous measurement of delay time larger than T, that is, the transmitted pulse width.

Taking into consideration that the transmitted pulse width is T, this ambiguity is removed by the range gates which are inserted after the envelope detector. These range gates have the same repetition frequency as that of the transmitted pulse and they are so arranged that their time differences are equal to the transmitted pulse width. Therefore the output of the first gate indicates the existence of the reflected signal with delay between 0 and T, and that of the second g gate indicates the existence of the reflected signal with delay between T and 2T and so forth.

The first threshold detector quantizes the output of envelope d detector into 0 or 1. The succeeding counter integrates the number of 1 during a certain time interval. If this number exceeds the second threshold, the alarm signal will be obtained. The double threshold method of detection made possible the application of digital technique to detection process and to stabilize the system by eliminating the various disturbances from the outsides.

Fig. 8 shows the waveforms involved in the detection process in case of zero time difference between the reflected signal and the local reference signal. These pictures are taken using the laboratory model, where the carrier frequency is 1.9 MC, the pulse repetition frequency is 100 c/s, pulse width 1 m sec and the pseudo-random sequence of length 15 is utilized as a modulating signal. The fifth order maximally-flat-delay L C filter with the 3 db bandwidth of 760 c/s and with the center frequency of 100 kc/s is used as a narrow band filter. According to the experiments, the doppler shifts of ±300 c/s cause a neglegible effects on the amplitude of the outputs. The doppler shifts of ±600 c/s give 6 db attenuation, and those of ±900 c/s are found to give practically zero output.

Fig. 9 shows the waveforms in case of nonzero time difference between the reflected signal and the local reference signal. This picture shows the imcomplete building up of the output waveform of a narrow band filter. For each time difference between the reflected and local signals, the observation was made resulting the ambiguity diagram shown in Fig. 10. In Fig. 10, the ordinate shows the relative amplitude of the output of the narrow band filter. The unit of k is one cycle of a feedback shift register. From these results, it is shown that the worst descrimination factor is 0.3. Over the wide range of k, the discrimination factor is better than 0.2. The peak at the origin indicates the true coordinate of a single target. Observe that the response falls off sharply from the origin. The theory shows that the sharpness of the peak depends on the band width of the modulating signal, that is, the bandwidth of the pseudo-random sequence. Increasing the maximal period of the pseudo-random sequence derived from a feedback shift register, the sharpness of the peak is increased indefinitely. For the specific pseudo-random signal with the length of 15, that is taken as an example, there appear spurious peaks at k=-7, k=5 and so forth. The magnitudes of these kinds of peaks are expected to decrease by employing a pseudo-random sequence with a larger maximal period. Furthermore, in practice the magnitude of the expected spurious peaks can be reduced by employing post-detection integration of successive radar responses. In that case the sharpness of the peak at the origin is also increased.

Fig. 11 shows the two dimensional ambiguity diagram of the RF pulse modulated by a pseudo-random signal of length 13. The doppler response that is, the response along the doppler axis is the familiar $\frac{\sin^2 x}{x^2}$ type. This agrees with the general property of ambiguity diagram which gives this type of response unless amplitude versus time weighting is employed.

It is again emphasized that these results represent the experimental results of the specific system response. By designing the waveform properly, the ambiguity diagram is expected to improve as far as its sharpness at the origin and the magnitudes of the spurious responses are concerned.

Maximum Range : Total Power

Range Resolution : Signal Bandwidth

Multiple Target Separation : Orthogonal Signal

Fig. 1 Required Radar Performances

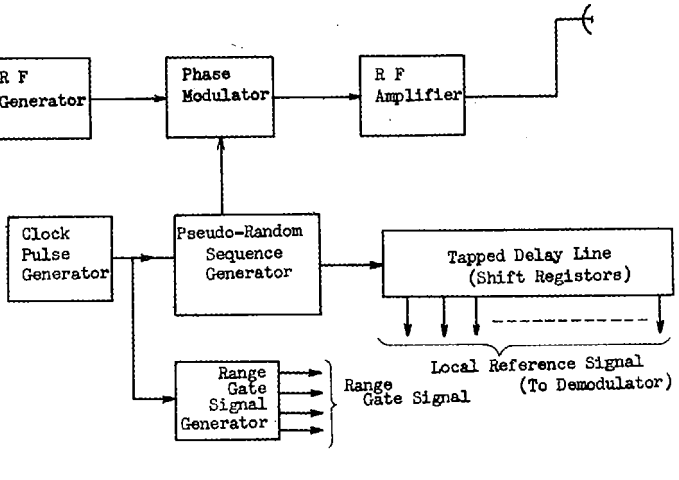

Fig. 2 Transmitter of Coded Pulse Radar

(A) Carrier Pulse

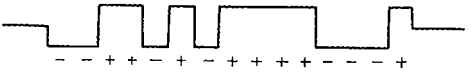

(B) Pseudo-Random Sequence Derived from Feedback shift Register

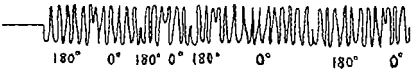

(C) Output of Modulator.

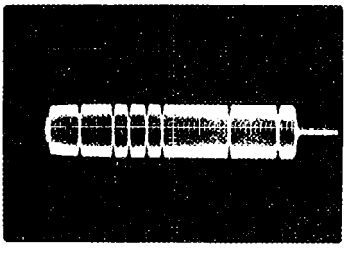

(D) Oscillographed Waveform

Fig. 3 Pseudo-Randomly Phase Modulated Pulse

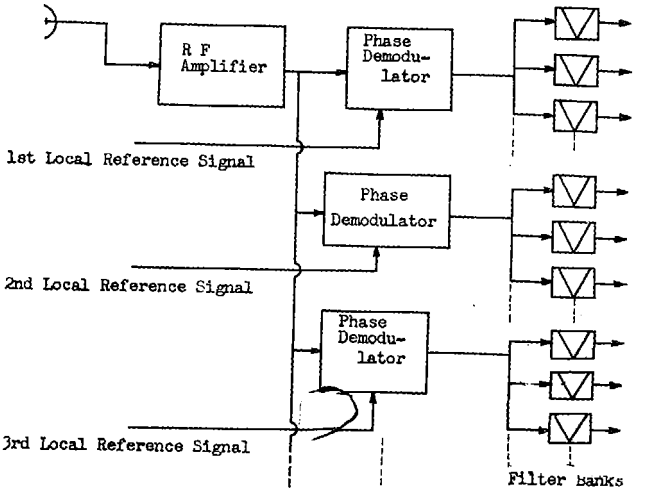

Fig. 4 Receiver of Coded Pulse Radar

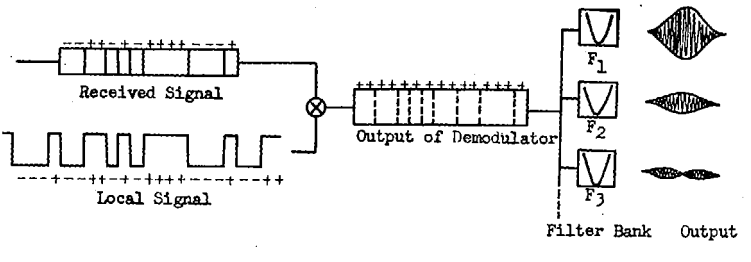

Fig. 5 Method of Correlation Detection I
(In case of Zero Delay)

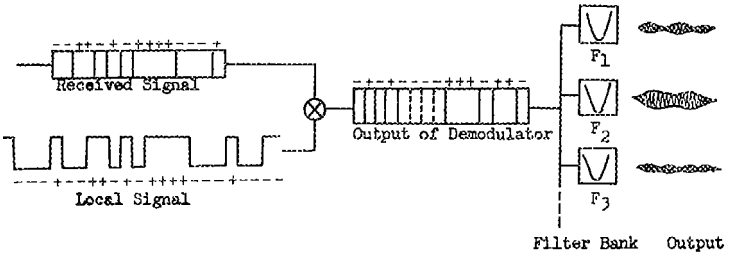

Fig. 6 Method of Correlation Detection II
(In case of Nonzero Delay)

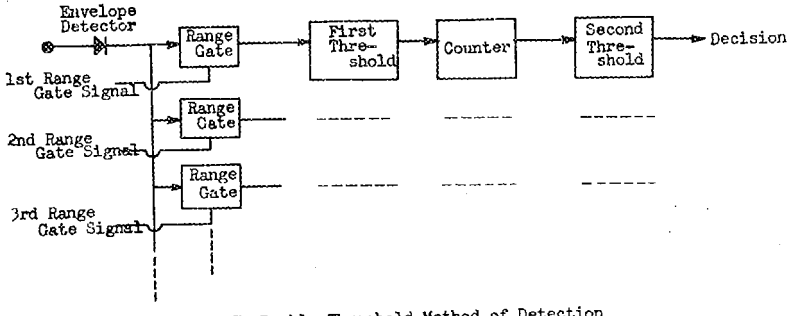

Fig. 7 Double Threshold Method of Detection

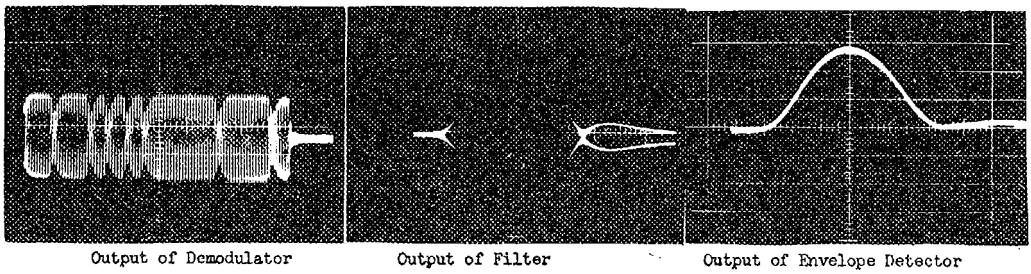

Fig. 8 Correlation Detection with Zero Delay

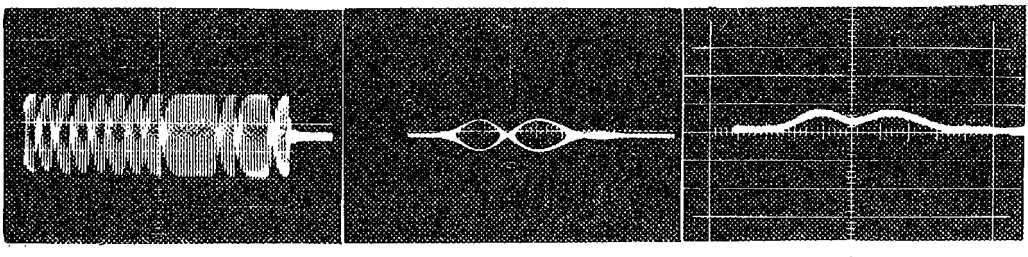

Fig. 9 Correlation Detection with Nonzero Delay

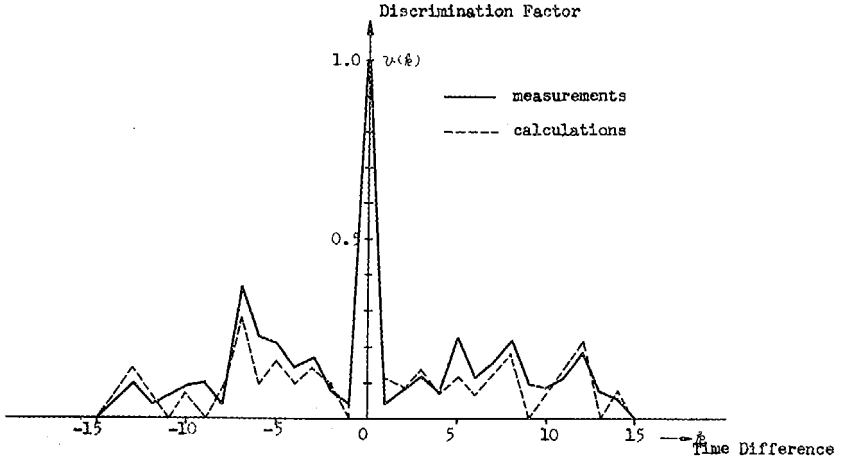

Fig. 10 Ambiguity Diagram
(Discrimination Factor Time Difference)

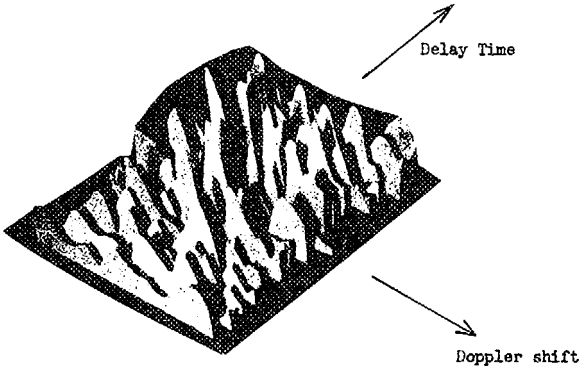

Fig. 11 Ambiguity Diagram (Experimental Results)
(Selectivity in Doppler Shift - Delay Time Plane)